Fast Prediction of Unbalanced Magnetic Pull in PM Machines

Seyed Payam Emami[1], Samad Taghipour Boroujeni[*1], Noureddine Takorabet[2]

1) Engineering Department, Shahrekord University, Shahrekord, Iran
2) GREEN, University of Lorraine, Nancy, France
*Correseponding author's email: s.taghipour@sku.ac.ir

In this work, a model is proposed for the computation of Unbalanced Magnetic Pull (UMP) in PM machines. This model is suitable for use in dynamic simulations. However, the aim of this research is not dynamic modeling of the PM machines. The main idea is to provide a fast model to be integrated into the dynamic models of PM machines. To reduce the required computational burden, the UMP of PM machines is expressed as a second-order algebraic vector function of the stator currents. The function parameters are estimated by post-processing of the results of some magneto-static simulations. These parameters are functions of the machine geometrical data and the rotor position. The role of these parameters in the computation of the machine UMP is the same as the role of the machine inductances in computation of the electromagnetic torque. To investigate the capability of the developed model, the UMP of a concentric fractional-slot surface PM machine with diametrically asymmetric stator windings, and the UMP of an eccentric PM-inset machine are predicted. The obtained results are compared in the terms of the consumed time and the accuracy by means of finite element analysis.

Index Terms— **Unbalanced magnetic pull, PM machines, fast prediction, parameter estimation.**

I. INTRODUCTION

USING electrical machines in a variety of applications is increasing day by day. Usually, Unbalanced Magnetic Pull (UMP) in electrical machines is an undesirable phenomenon that causes vibration, acoustic noise, and a chain of damages in the bearings [1-3]. UMP may occur in faulty machines such as the machines with the rotor eccentricity [4-9] or with the magnet imperfection [9-11]. In addition, manufacturing tolerances may result in UMP [4]. Even UMP may appear in healthy machines such as the fractional-slot machines with diametrically asymmetric stator windings [12-14], multi-sector three-phase machines [15], and the magnetic gears [10]. However, UMP is not always an undesirable effect. In magnetic bearing [17] and bearingless PM machines [18], the radial force is used for the rotor magnetic levitation. Therefore, the UMP computation is an important and interesting issue in the analysis of electrical machines. As a numerical method, Finite Element Analysis (FEA) is an accurate method for the computation of UMP [2, 19-21]. However, FEA includes time-consuming computations. Therefore, it is not an efficient tool for the first step design of the electrical machines. The machine UMP could be computed by using analytical models and applying the Maxwell stress definition. Using the analytical models, the machine UMP is computed for the Surface PM (SPM) with concentric [12-15,18] and eccentric [4-11] rotors, eccentric PM-inset machines [5] and the reluctance synchronous machines [22]. The effect of the circumferential magnetic field in the radial magnetic pressure is neglected in [22], while it is considered in [3-18]. In [19-24], the harmonic spectrum of UMP is predicted by using the Maxwell stress definition. In the proposed models for UMP [3-24], the exact distribution of the air gap flux density components is required. This issue is a ban for using these model in time-stepping simulations because in each time interval of the Runge–Kutta computations of dynamic simulations, the magnetic flux density of all points of the considered Maxwell surface in the air gap must be computed and it increases drastically the computational burden of

dynamic simulations. On the other hand, exact knowledge of the flux density distribution is out of interest in the dynamic studies. Although some techniques could be used to speed up the field computation models [25], they are still too slow to be used in the dynamic simulations for computation of UMP.

To fill the existing gap for the fast UMP computation in PM machines, a model is proposed in this work that is fast enough to be applied in the dynamic simulations. To reduce the required computational burden, the UMP of PM machines is expressed as a second-order algebraic vector function of the stator currents in II. This function is obtained by using the Maxwell stress definition. The parameters of this function are obtained as functions of the rotor position and the machine geometry by post-processing the results of the magneto-static simulations of PM machines in III. These parameters are obtained for a predefined number of rotor positions and could be used as lookup tables in dynamic simulations. These parameters are defined for the first time and their role in the computation of UMP is the same as the role of the machine inductances in the computation of electromagnetic torque.

The aim of this paper is neither the magneto-static analysis nor the dynamic modeling of PM machines. The intended idea is providing the machine UMP as an instantaneous vector function of the machine currents. Therefore, to save space, the modeling process of the air gap flux density is not included, and the distribution of air gap flux density is found by using the existing magneto-static models in the literature. In addition, the developed UMP model is not integrated as a part of the dynamic model of the electrical machines. The performance of the proposed approach for the prediction of the machine UMP is investigated for some predefined current waveforms in two PM machines. The considered machines are a concentric fractional-slot SPM machine with diametrically asymmetric stator windings, and an eccentric PM-inset machine. Finally, the accuracy and efficacy of the proposed model are evaluated by comparing the results with FEA.
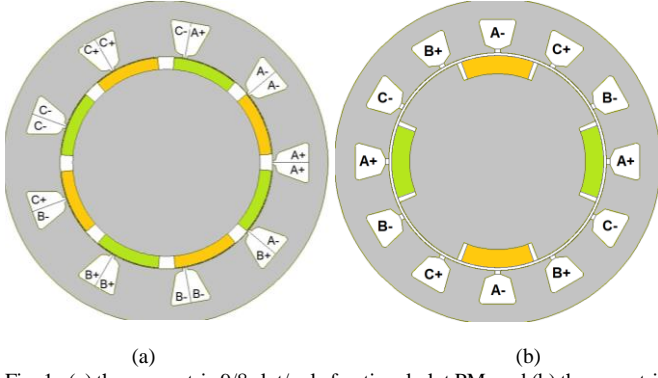
Fig. 1. (a) the concentric 9/8 slot/pole fractional-slot PM, and (b) the eccentric PM-inset concentric PM machines.

Parameter	SPM	PM-inset
pole pairs	4	2
Stator bore	63 mm	30 mm
Air gap length	0.5 mm	0.75 mm
Rotor radius	59.5 mm	24.25 mm
The PM arc to the pole pitch	0.8	0.56
The Rotor slot arc to the pole pitch	---	0.7
PM remanent flux density	0.3 T	1.2 T
Machine stack length	40 mm	60 mm
The coils' turn number	150	20
Type of the stator winding	double-layer	single-layer
Slot opening	3mm	2mm
No. the stator coils per phase	3	2

II. MODELING OF THE UMP

Based on the Maxwell stress tensor definition, the machine UMP is obtained as given in (1)

$$\mathbf{F} = F_x + jF_y =$$

$$\frac{RL_{stk}}{2\mu_0} \int_0^{2\pi} \left(\left(B_r^2 - B_\varphi^2 \right) + j\, 2B_r B_\varphi \right) e^{j\varphi} d\varphi \tag{1}$$

where, B_r and B_φ are the resultant radial and circumferential components of the air gap flux density, respectively, R is the radius of Maxwell cylindrical surface, L_{stk} is the machine stack length and μ_0 is the air permeability. It is worth mentioning that the real and imaginary parts of $\mathbf{F}$ are responsible for the x and y components of UMP. Neglecting magnetic saturation and applying the superposition theorem, the air gap flux density components are decomposed to the armature current and the PMs as expressed in (2), where the subscripts "PM" and "AR" are responsible for PMs and armature currents, respectively.

$$B_r = B_{rPM} + B_{rAR}$$
$$B_\varphi = B_{\varphi PM} + B_{\varphi AR} \tag{2}$$

It is useful to substituting (2) into (1) and decomposing the UMP expression into three terms as given in (3).

$$\mathbf{F} = \mathbf{F_{PM}} + \mathbf{F_{Ar}} + \mathbf{F_{PMAr}} \tag{3}$$

where,

$$\mathbf{F_{PM}} = \frac{RL_{stk}}{2\mu_0} \int_0^{2\pi} \left(B_{rPM}^2 - B_{\varphi PM}^2 + 2jB_{rPM} B_{\varphi PM} \right) e^{j\varphi} d\varphi \tag{4}$$

$$\mathbf{F_{AR}} = \frac{RL_{stk}}{2\mu_0} \int_0^{2\pi} \left(B_{rAR}^2 - B_{\varphi AR}^2 + 2jB_{rAR} B_{\varphi AR} \right) e^{j\varphi} d\varphi \tag{5}$$

$$\mathbf{F_{PMAR}} = \frac{RL_{stk}}{\mu_0} \int_0^{2\pi} \left(B_{rAR} B_{rPM} - B_{\varphi AR} B_{\varphi PM} \right) e^{j\varphi} d\varphi$$
$$+ \frac{jrL_{stk}}{\mu_0} \int_0^{2\pi} \left(B_{rAR} B_{\varphi PM} + B_{rPM} B_{\varphi AR} \right) e^{j\varphi} d\varphi \tag{6}$$

The term $\mathbf{F_{PM}}$ in (4) is the UMP caused only by the PMs. This term depends only on the rotor position, θ_r, and is independent of the armature currents as expressed in (7). This term of UMP exists in the eccentric PM machines [4-9], concentric machines with PM imperfection [9-11], and PM machines with asymmetric armature winding [12-14].

$$\mathbf{F_{PM}} = \boldsymbol{\delta}(\theta_r) \tag{7}$$

The term $\mathbf{F_{AR}}$ in (5) is only due to the armature reaction field, and the term $\mathbf{F_{PMAR}}$ is due to the interaction of the PMs and the armature field. The terms $\mathbf{F_{AR}}$ and $\mathbf{F_{PMAR}}$ are functions of the armature currents and the rotor position. As seen in (4)-(6), exact knowledge of the distribution of the air gap flux density components is required for computing the machine UMP. Neglecting the magnetic saturation, the armature flux density is a linear combination of the phase currents (i_a, i_b, and i_c) as expressed in (8).

$$\begin{bmatrix} B_{rAR}(r,\varphi,\theta_r) \\ B_{\varphi AR}(r,\varphi,\theta_r) \end{bmatrix} = \mathbf{K}(r,\varphi,\theta_r) \begin{bmatrix} i_a \\ i_b \\ i_c \end{bmatrix} \tag{8}$$

$$\mathbf{K} = \begin{bmatrix} K_{ar}(r,\varphi,\theta_r) & K_{br}(r,\varphi,\theta_r) & K_{cr}(r,\varphi,\theta_r) \\ K_{a\varphi}(r,\varphi,\theta_r) & K_{b\varphi}(r,\varphi,\theta_r) & K_{c\varphi}(r,\varphi,\theta_r) \end{bmatrix}$$

where, r and φ are respectively the radial and circumferential variables of the desired point of the air gap, respectively. The elements of the matrix $\mathbf{K}$ are the coefficients of the armature currents. These elements are dependent on machine dimensions. In the other words, $K_{xr}(r,\varphi,\theta_r)/K_{x\varphi}(r,\varphi,\theta_r)$ is the radial/circumferential flux density component in the desired point of the air gap at the rotor position θ_r with 1A in phase x and open circuit condition in the other phases, where $x\epsilon\{a,b,c\}$. In contrast to the salient PM machines (PM-inset and interior PM machines) and eccentric SPM machines, in the concentric SPM machines, K_{xr} and $K_{x\varphi}$ are independent of θ_r. Considering the air gap flux density components in (8) and substituting them into (5) and (6), the terms $\mathbf{F_{AR}}$ and $\mathbf{F_{PMAR}}$ are obtained in (9) and (10), respectively.

$$\mathbf{F_{AR}} = \boldsymbol{\alpha}_a(\theta_r)i_a^2 + \boldsymbol{\alpha}_b(\theta_r)i_b^2 + \boldsymbol{\alpha}_c(\theta_r)i_c^2 + \boldsymbol{\beta}_{ab}(\theta_r)i_a i_b + \boldsymbol{\beta}_{bc}(\theta_r)i_b i_c + \boldsymbol{\beta}_{ac}(\theta_r)i_a i_c \tag{9}$$

$$\mathbf{F_{PMAR}} = \boldsymbol{\gamma}_a(\theta_r)i_a + \boldsymbol{\gamma}_b(\theta_r)i_b + \boldsymbol{\gamma}_c(\theta_r)i_c \tag{10}$$

where, $\boldsymbol{\alpha}$, $\boldsymbol{\beta}$ and $\boldsymbol{\gamma}$ are the coefficients of the UMP function. Hereafter, the coefficients of the UMP function are estimated by post-processing of the magneto-static results of the PM machines. The magneto-static results could be obtained by applying analytical models or FEA. It is worth mentioning that the type of the PM machine including its geometry and its stator (slotted/slotless one) are not limiting issues in the proposed model.

In analysis of the PM machines by using time-stepping FEA or using the previously proposed analytical models, for
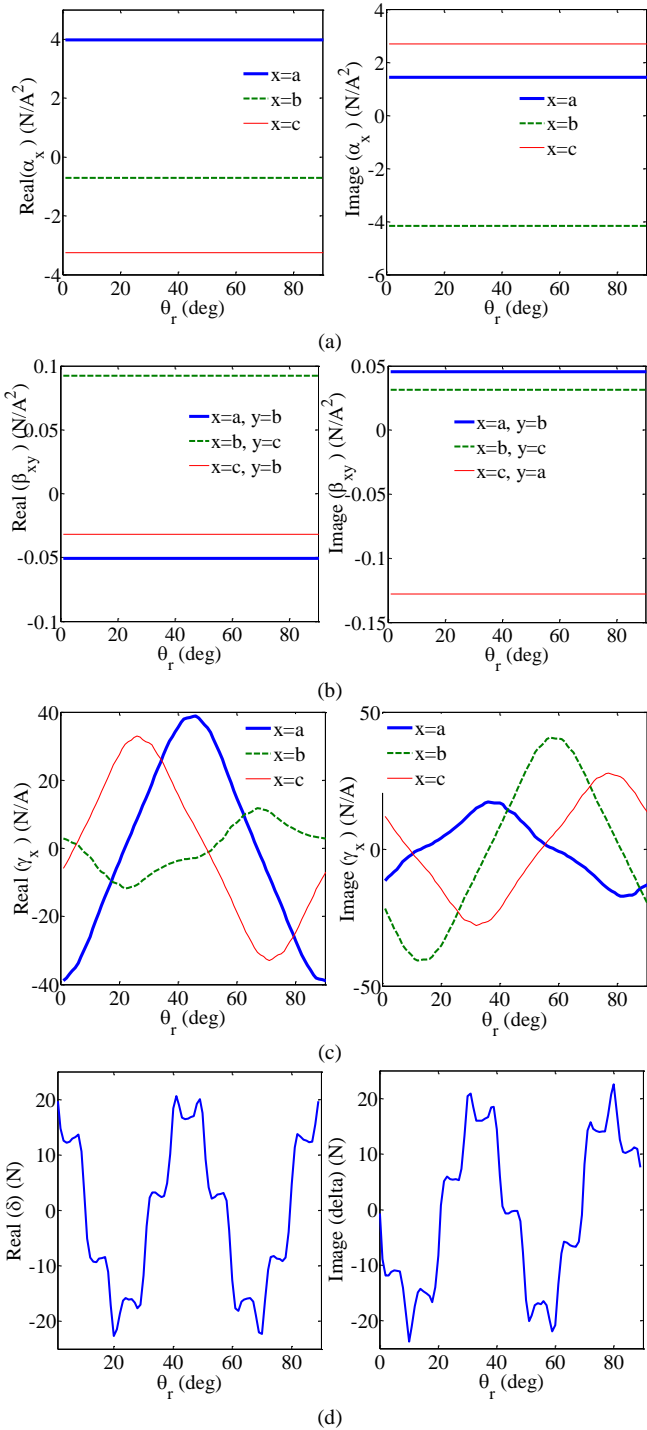
Fig. 2. The real and imaginary parts of the variables (a) **α**, (b) **β**, (c) **γ** and **δ** for the UMP of the concentric 9-slot 8-pole fractional-slot SPM machine versus the rotor position.

computation of UMP the following items must be carried out in each time-step of the simulation.

- Finding the current in the case of having voltage sources as the excitation by solving Runge–Kutta algorithms.
- Computation of the flux density distribution by knowing the rotor position and the currents.
- Using Maxwell stress integration to find UMP.
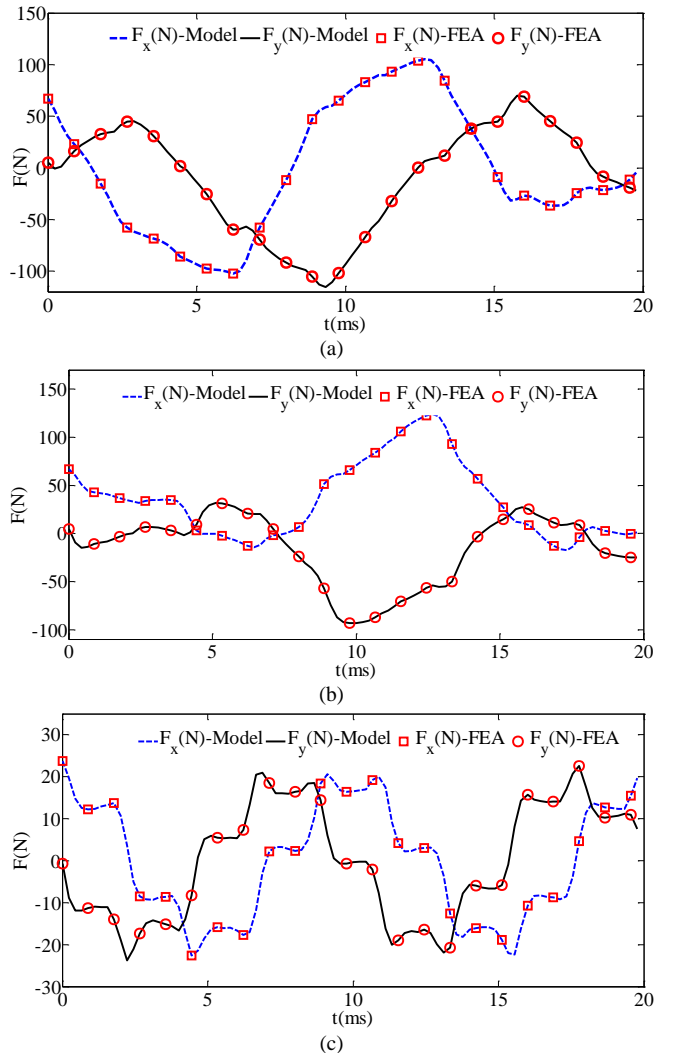
Fig. 3. The UMP components of the concentric fractional slot SPM machine with (a) three-phase balanced and (b) two-phase unbalanced current excitation, and (c) no-load condition.

In contrast, in the presented approach it is not required to carry out above steps. Knowing the currents, it is just enough to use the presented static function (3) for computation of UMP. The coefficients of the presented UMP function are obtained only one time for predefined discrete rotor positions by using (FEA or an analytical model), and used as lookup tables for computation of UMP in future computations. In the case that the exact value of the desired rotor position in one time-step is not found in the lookup interpolation must be applied.

III. PARAMETER ESTIMATION

The parameter $\delta(\theta_r)$ is obtained from the data of the no-load simulation as given in (7). The coefficients **α**, **β,** and **γ** could be obtained directly by knowing the exact distribution of the armature air gap flux density components. Applying (8) into (5) and (6), the parameters **α**, **β,** and **γ** yield as (11)-(13), respectively.
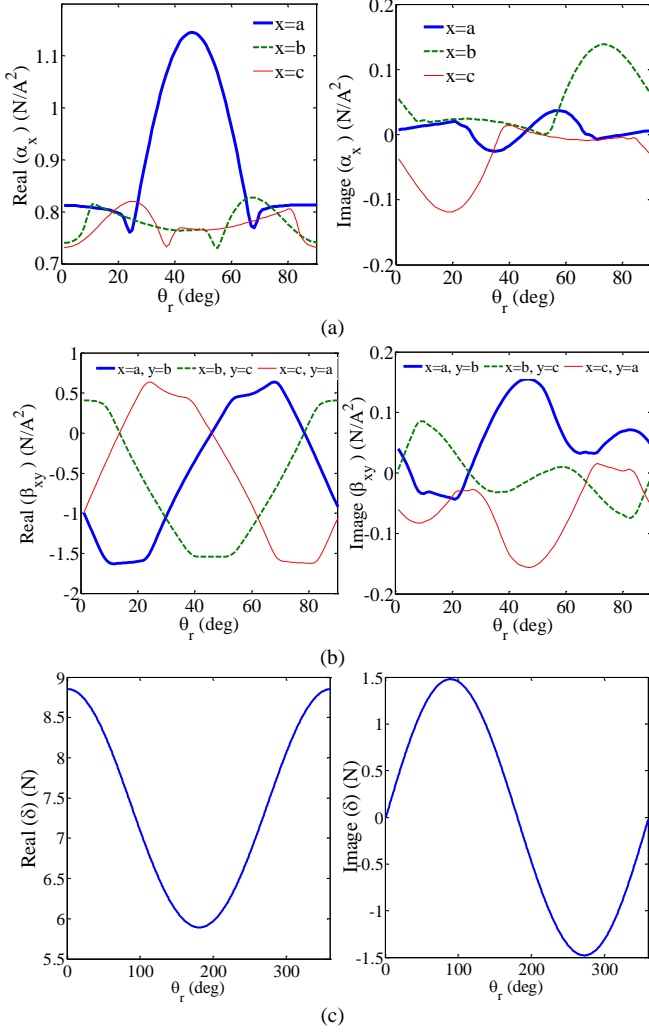
Fig. 4. The real and imaginary parts of the variables (a) **α**, (b) **β**, and (c) **δ** for the UMP of the eccentric PM-inset machine versus the rotor position.

$$\boldsymbol{\alpha}_x(\theta_r) =$$

$$\frac{RL_{stk}}{2\mu_0}\int_0^{2\pi}\left(K_{xr}^2 - K_{x\varphi}^2 + 2jK_{xr}K_{x\varphi}\right)e^{j\varphi}d\varphi \qquad (11)$$

$$\boldsymbol{\beta}_{xy}(\theta_r) =$$

$$\frac{RL_{stk}}{\mu_0}\int_0^{2\pi}\left(K_{xr}K_{yr} - K_{x\varphi}K_{y\varphi}\right)e^{j\varphi}d\varphi \qquad (12)$$

$$j\,\frac{RL_{stk}}{\mu_0}\int_0^{2\pi}\left(K_{xr}K_{y\varphi} + K_{yr}K_{x\varphi}\right)e^{j\varphi}d\varphi$$

$$\boldsymbol{\gamma}_x(\theta_r) =$$

$$\frac{RL_{stk}}{\mu_0}\int_0^{2\pi}\left(K_{xr}B_{rPM} - K_{x\varphi}B_{\varphi PM}\right)e^{j\varphi}d\varphi \qquad (13)$$

$$+j\,\frac{RL_{stk}}{\mu_0}\int_0^{2\pi}\left(K_{xr}B_{\varphi PM} + K_{x\varphi}B_{rPM}\right)e^{j\varphi}d\varphi$$

In this method, four independent analyses of four simulations magneto-static analysis have to be carried out. The simulations are as: 1) the no-load simulation with only PM excitation, 2) $i_a=1A$, $i_b=i_c=0$, 3) $i_a=0$, $i_b=1A$, $i_c=0$, and 4) $i_a=i_b=0$, $i_c=1A$. It is worth mentioning that, in the concentric machines, it is
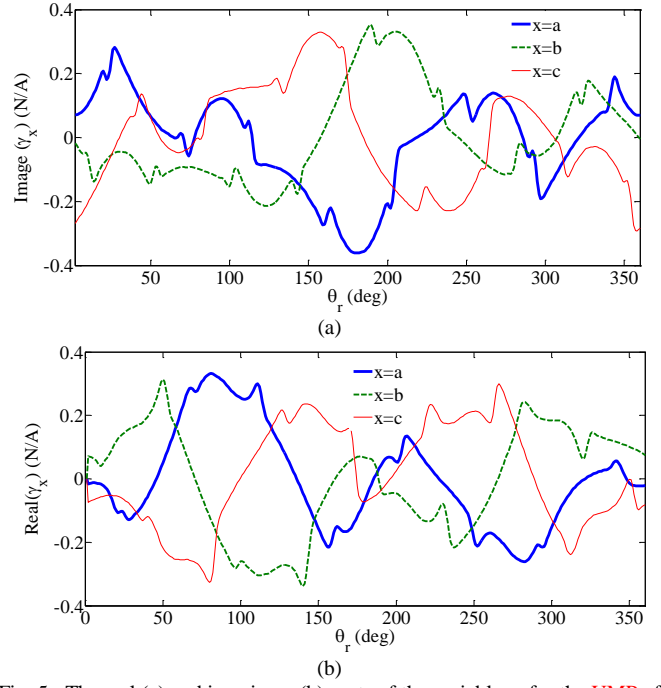
Fig. 5. The real (a) and imaginary (b) parts of the variable γ, for the UMP of the eccentric PM-inset machine versus the rotor position
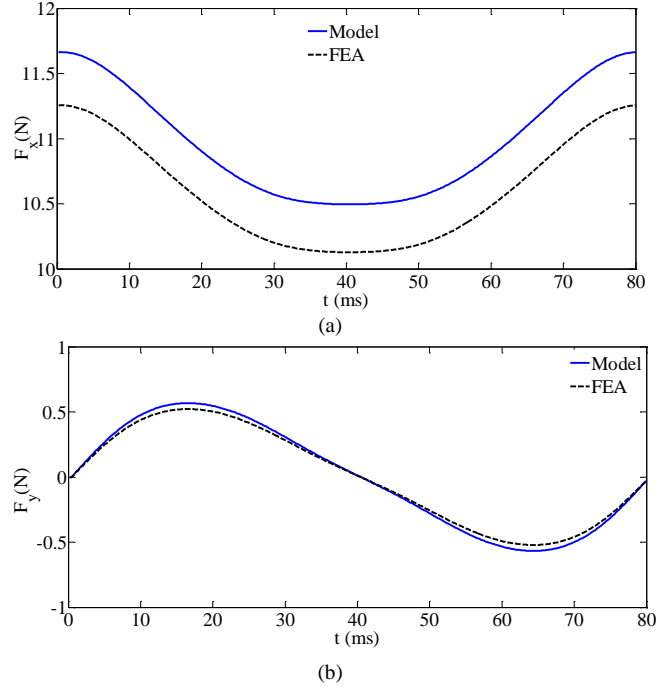
Fig. 6. The (a) x- and (b) y- components of UMP of the eccentric PM-inset machine versus the rotor position at no-load condition.

expected that the waveforms of the parameters **α**, **β**, and **γ** in one phase be the same as the other phases with the angular shift of 2π/3 rad. as expressed in (14).

$$\boldsymbol{\alpha}_a(\theta_r) = \boldsymbol{\alpha}_b(\theta_r)e^{j\frac{2\pi}{3}} = \boldsymbol{\alpha}_c(\theta_r)e^{j\frac{4\pi}{3}}$$

$$\boldsymbol{\beta}_{ab}(\theta_r) = \boldsymbol{\beta}_{bc}(\theta_r)e^{j\frac{2\pi}{3}} = \boldsymbol{\beta}_{ca}(\theta_r)e^{j\frac{4\pi}{3}} \qquad (14)$$

$$\boldsymbol{\gamma}_a(\theta_r) = \boldsymbol{\gamma}_b(\theta_r)e^{j\frac{2\pi}{3}} = \boldsymbol{\gamma}_c(\theta_r)e^{j\frac{4\pi}{3}}$$
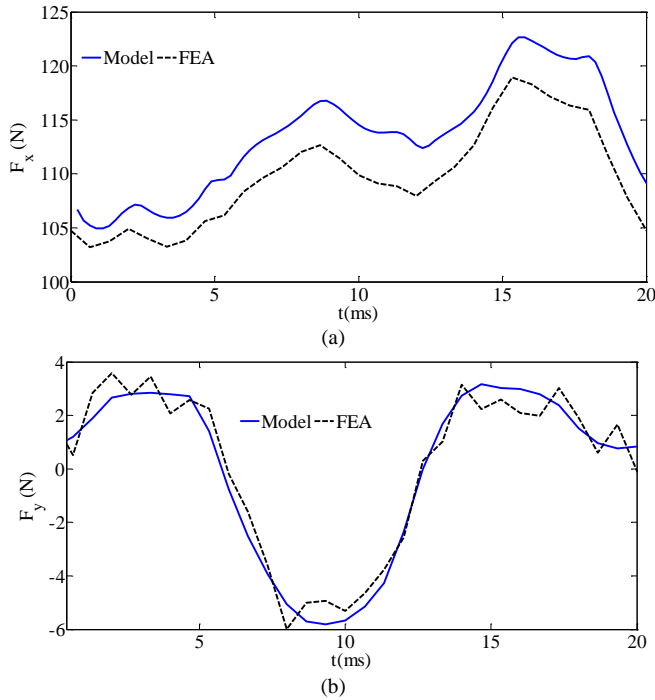
Fig. 7. The UMP (a) x and (b) y components for the three-phase balanced currents in the eccentric PM-inset machine.

Fig. 8. The UMP (a) x and (b) y components for two-phase currents in the eccentric PM-inset machine.

IV. CASE STUDY AND MODEL VERIFICATION

To investigate the applicability of the developed model for the prediction of the machine UMP, two types of PM machines are studied. One machine is a fractional-slot SPM machine with diametrically asymmetric stator windings and a concentric rotor, and the other one is PM-inset with an integral-slot stator winding and eccentric rotor. These machines are shown in Fig.1 (a) and (b), respectively. The machines' data are reported in Table I. Since the aim of this paper is not the magneto-static analysis, the approach of finding the air gap flux density is not reported to save space. The magneto-static-models in [4] and [5] are used for the air gap flux density computation in the SPM and PM-inset machines, respectively. The main idea is providing the machine UMP as an instantaneous function of the machine currents and the rotor position. Therefore, the performance of the proposed approach for the prediction of the machine UMP is investigated for some predefined current waveforms. The considered current waveforms are considered in the following conditions;

- The balanced three-phase current excitation.
- Sinusoidal current in two phases and open circuit in the other phase.

A. Fractional slot SPM machine

Since the machine periodicity in the 9-slot 8-pole fractional-slot PM machine is unit, there is some amount of F_{PM-AR}. In addition, since the phase windings are diametrically asymmetric, depends on the phases excitation some amount of F_{AR} may be generated. Although the PM machine is concentric structure, due to diametrically asymmetric stator slots F_{PM} and consequently the parameter δ is not zero. The stator winding layout is shown in Fig.1 (a). The model in [5] is used for the
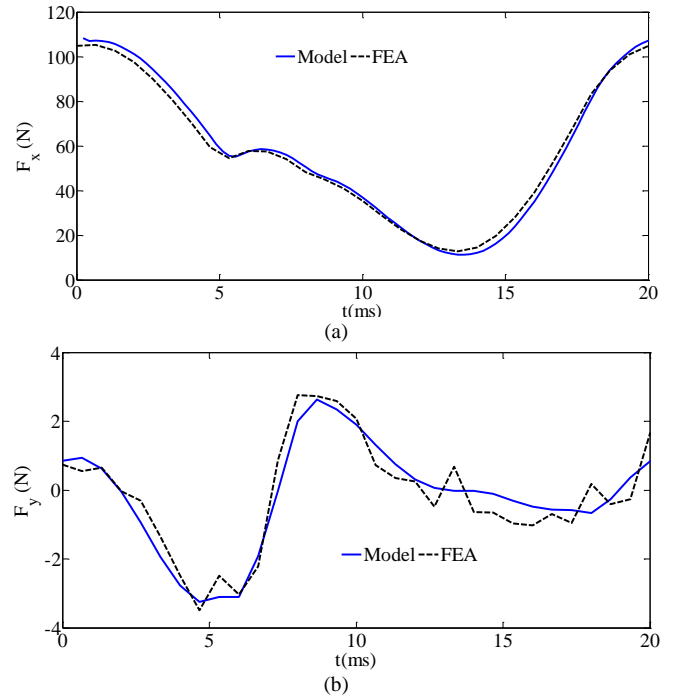
prediction of the air gap flux density components and the effects of the slots are considered. The parameters α, β, γ and δ are obtained and shown in Fig.2. Since the variables period is 90°, the curves are shown only for 90° of the rotor position interval. As expected due to the concentric rotor, the UMP parameters of the phases satisfy (14). However, due to the large air gap seen by the armature windings F_{AR} and its related coefficients, i.e. α and β, are very small. Although α and β are constant due to the uniform air gap, the coefficients γ and δ depend on the rotor position. It could be stated that the force is almost due to the interaction between the armature and the PMs. It should be noted that the zero rotor position is shown in Fig.1 (a).

A three-phase balanced current with an amplitude of 5A rms and frequency of 50Hz is applied to the stator and the obtained UMP components are illustrated and compared with FEA results in Fig.3 (a). In another test, the phase currents are considered as (15) and the UMP components are obtained and compared with FEA in Fig.3 (b). The no-load UMP waveform is shown in Fig.3 (c). It should be noted that the UMP waveforms in Fig.3 are obtained in synchronous rotor speed.

$$i_a(t) = 5\sqrt{2}\cos(100\pi t) \text{ Amp.}$$
$$i_b(t) = -5\sqrt{2}\cos(100\pi t) \text{ Amp.} \tag{15}$$
$$i_c(t) = 0 \text{ Amp.}$$

As seen in Fig. 3, the model predicted results are the same as the FEA results. The required time for computation of the machine UMP in a single rotor position is 90 µsec., 32 msec. and 6.2sec. for the proposed model, analytical magneto-static and FEA approaches. Therefore, the proposed model is the fastest and more suitable one for use in dynamic simulations.

B. Eccentric PM-inset machine

In the eccentric PM-inset machine, all three UMP components in (3) are non-zero. Zero rotor position and the stator winding layout of this machine are shown in Fig.1 (b). In addition, the static rotor eccentricity with 70% of the air gap length is applied and the proposed analytical model in [5] is used for the magneto-static simulations. Analyzing the results of the carried out magneto-static simulations, the parameters α, β, and δ are obtained as functions of the rotor position and shown in Fig.4 (a)-(c), respectively. The real and imaginary parts of γ are shown in Fig.5 (a) and (b).

Since the air gap in the PM-inset machine is small and salient, in comparison with the SPM machines, the parameters α and β are dependent on the rotor position. In addition, since the static rotor eccentricity condition is considered, the waveforms of the variables in different phases do not satisfy (14).

The no-load UMP waveform of the considered eccentric PM-inset machine is shown in Fig.6. A three-phase balanced current with an amplitude of 5A rms and frequency of 50Hz is applied to the stator and the obtained UMP components are illustrated and compared with FEA results in Fig.7 (a) and (b). In another test, the phase currents are considered as (15) and the UMP components are obtained and compared with FEA in Fig.8 (a) and (b). It should be noted that the UMP waveforms in Figs.6-8 are obtained in synchronous rotor speed.

The required time for computation of the UMP in the PM-inset machine in a single rotor position 90 µsec., 43 msec. and 8.7 sec. for the proposed model, analytical magneto-static in [5] and FEA approaches. Therefore, the proposed model is the fastest and more suitable one for using in the dynamic simulations.

As seen in Figs. 3, 6,7, and 8, there is a good agreement between the provided model results and FEA in predicting the machine UMP. However, in the developed model, the UMP components are expressed as the second-order instantaneous functions of the stator current, while in the existing approaches it is needed to obtain the flux density components on the considered Maxwell surface and applying the integration operator which requires time and more computational burden.

V. CONCLUSION

In the presented paper, the machine UMP is expressed as a second-order algebraic function of the armature currents. Although the model is valid for all types of PM machines or even the synchronous reluctance ones, with no loss of generality only SPM and PM-inset machines are studied. The parameters of the proposed UMP function are obtained by post-processing of four number of the magneto-static simulations at every single rotor position. The magneto-static analysis could be carried out by applying the analytical models or FEA. The UMP parameters are obtained for a predefined number of rotor positions and could be used as lookup tables in dynamic simulations. Finally, two cases of having UMP, i.e., a concentric fractional-slot SPM machine with diametrically asymmetric stator windings and an eccentric PM-inset machine

with predefined current waveforms are studied. The current waveforms are selected for two conditions of three-phase balanced excitation and one open-circuited phase condition. The obtained UMP components are compared and verified by means of FEA.

REFERENCES

[1] J. Krotsch, B. Piepenbreier, "Radial Forces in External Rotor Permanent Magnet Synchronous Motors With Non-Overlapping Windings," IEEE Trans. Ind. Elec., vol. 59, no. 5, May 2012, pp. 2267-2276

[2] T. Yoon, "Magnetically induced vibration in a permanent-magnet brushless DC motor with symmetric pole-slot configuration," IEEE Trans. Magn., vol. 41, no. 6, June 2005, pp. 2173-2179

[3] Z. Q. Zhu, M. L. M. Jamil, and L. J. Wu, "Analytical Modeling and Finite-Element Computation of Radial Vibration Force in Fractional-Slot Permanent-Magnet Brushless Machines," IEEE Trans. Ind. Appl., vol. 46, no. 15, Sep./OCt. 2010, pp. 1908-1918

[4] S. T. Boroujeni, P. Jalali, N. Bianchi, "Analytical modeling of no-load eccentric slotted surface mounted PM machines: cogging torque and radial force," IEEE Trans. Magn., vol. 30, no. 2, June 2015, pp. 754–760.

[5] S. T. Boroujeni, S. P. Emami, and P. Jalali, "Analytical Modeling of Eccentric PM-inset machines with a Slotless Armature," IEEE Trans. Energy Convers., vol.34, no.3, Sep. 2019, pp.1466-1474.

[6] R. Goraj "Prediction of the static unbalanced magnetic pull in synchronous surface mounted permanent magnet machines," Electrical Engineering, Vol. 99, pages 861–869, 2017.

[7] F. Boy and H. Hetzler, "An asymptotic approximation of the magnetic field and forces in electrical machines with rotor eccentricity," Electrical Engineering, Vol. 100, pp. 389–399, 2018

[8] J. T. Li, Z. J. Liu, and L. H. A. Nay, "Effect of Radial Magnetic Forces in Permanent Magnet Motors With Rotor Eccentricity," IEEE Trans. Magn., vol. 43, no. 6, June 2007, pp. 2525-2527

[9] J. Y. Song, K. J. Kang, C. H. Kang, and G. H. Jang, "Cogging Torque and Unbalanced Magnetic Pull Due to Simultaneous Existence of Dynamic and Static Eccentricities and Uneven Magnetization in Permanent Magnet Motors," IEEE Trans. Magn., vol. 53, no. 3, March 2017, ASN. 8200609

[10] H. Qian, H. Guo, Z. Wu, and X. Ding, "Analytical Solution for Cogging Torque in Surface-Mounted Permanent-Magnet Motors with Magnet Imperfections and Rotor Eccentricity," IEEE Trans. Magn., vol. 50, no. 8, Aug. 2014, Article ID.8201615

[11] A. J. P. Ortega, and L. Xu, "Investigation of Effects of Asymmetries on the Performance of Permanent Magnet Synchronous Machines," IEEE Trans. Energy Convers., vol. 32, no. 3, Sep. 2017, pp. 1002-1011

[12] P. Jalali, S. T. Boroujeni, J. Khoshtarash, "Expansion of the feasible slot/pole combinations in the fractional slot PM machines by applying three-slot pitch coils," IEEE Trans. Energy Covers., vol. 34, no. 2, June 2019, pp. 993-999.

[13] Z. Q. Zhu, M. L. M. Jamil, and L. J. Wu, "Influence of Slot and Pole Number Combinations on Unbalanced Magnetic Force in PM Machines With Diametrically Asymmetric Windings," IEEE Trans. Ind. Appl., vol. 49, no. 1, Jan./Feb. 2013, pp. 19-30.

[14] Z. Q. Zhu, D. Ishak, D. Howe, and J. Chen, "Unbalanced Magnetic Forces in Permanent-Magnet Brushless Machines with Diametrically Asymmetric Phase Windings," IEEE Trans. Ind. Appl., vol. 34, no. 6, Nov./Dec. 2007, pp. 1544-1553

[15] G. Dajaku, "Advanced multi-phase fractional slot concentrated windings: characteristics and potentials," has been accepted for publication in Journal of Electrical Engineering-Springer.

[16] A. Rahideh, A. Vahaj, M. Mardaneh, and T. Lubin, "Two-dimensional analytical investigation of the parameters and the effects of magnetisation patterns on the performance of coaxial magnetic gears," IET Electr. Power Appl., vol. 3, Sep. 2017, pp. 230–245.

[17] F. Shakibapour, A. Rahideh, M. Mardaneh, "Two-dimentional analytical model for heteropolar active magnetic bearings considering eccentricity," IET Electr. Power Appl., vol. 12, no.5, May 2018, pp. 614–626.

[18] B. Lapôtre, N. Takorabet, F. Meibody-Tabar, J. Fontchastagner, R. Lateb, and J. D. Silva, "New Model of Radial Force Determination in Bearingless Motor," IEEE Trans. Magn., vol. 51, no. 3, Mach. 2015, Article ID. 8202104

[19] D. G. Dorrell, M. Popescu, and D. Ionel. "Unbalanced Magnetic Pull due to Asymmetry and Low-Level Static Rotor Eccentricity in Fractional-Slot

Brushless Permanent-Magnet Motors with Surface-Magnet and Consequent-Pole Rotors", IEEE Trans. on Magn. vol. 46, no.7, July 2010, pp. 2675-2685.

[20] D. G. Dorrell, M. F. Hsieh, and Y. G. Gu, "Unbalanced Magnet Pull in Large Brushless Rare-Earth Permanent Magnet Motors With Rotor Eccentricity," IEEE Trans. on Magn. vol. 45, no.10, Oct. 2009, pp. 4586-4589.

[21] D. G. Dorrell, J. K. H. Shek and M. F. Hsieh, "The Development of an Indexing Method for the Comparison of Unbalanced Magnetic Pull in Electrical Machines," IEEE Trans. on Ind. App.. vol. 52, no.1, Jan./Feb. 2016, pp. 145-153.

[22] H. Mahmoud, and N. Bianchi, "Eccentricity in Synchronous Reluctance Motors-Part I: Analytical and Finite-Element Models," Trans. Energy Convers., vol. 30, Issue 2, June 2015, pp. 745–753.

[23] L. J. Wu, Z. Q. Zhu, J. T. Chen, and Z. P. Xia, "An Analytical Model of Unbalanced Magnetic Force in Fractional-Slot Surface-Mounted Permanent Magnet Machines," IEEE Trans. Magn., vol. 46, no. 7, July 2010, pp. 2686-2700

[24] G. Dajaku and D. Gerling, "The Influence of Permeance Effect on the Magnetic Radial Forces of Permanent Magnet Synchronous Machines," IEEE Trans. Magn., vol. 49, no. 6, June 2013, pp. 2953-2966

[25] B. Hannon, P. Sergeant, and L. Dupre, "Computational-time reduction of Fourier-Based Analytical Models," IEEE Trans. Energy Convers., vol. 33, no 1, March 2018, pp. 281–289.